



UNIVERSITY OF LEEDS

This is a repository copy of *Orientation of a Diagnostic Ligand Bound to Macroscopically Aligned Amyloid- β Fibrils Determined by Solid-state NMR*.

White Rose Research Online URL for this paper:
<http://eprints.whiterose.ac.uk/138690/>

Version: Accepted Version

Article:

Townsend, D, Hughes, E, Stewart, KL et al. (3 more authors) (2018) Orientation of a Diagnostic Ligand Bound to Macroscopically Aligned Amyloid- β Fibrils Determined by Solid-state NMR. *Journal of Physical Chemistry Letters*, 9 (22). pp. 6611-6615. ISSN 1948-7185

<https://doi.org/10.1021/acs.jpcclett.8b02448>

This document is the Accepted Manuscript version of a Published Work that appeared in final form in *Journal of Physical Chemistry Letters*, copyright © 2018 American Chemical Society after peer review and technical editing by the publisher. To access the final edited and published work see [insert ACS Articles on Request author-directed link to Published Work, see <https://doi.org/10.1021/acs.jpcclett.8b02448>

Reuse

Items deposited in White Rose Research Online are protected by copyright, with all rights reserved unless indicated otherwise. They may be downloaded and/or printed for private study, or other acts as permitted by national copyright laws. The publisher or other rights holders may allow further reproduction and re-use of the full text version. This is indicated by the licence information on the White Rose Research Online record for the item.

Takedown

If you consider content in White Rose Research Online to be in breach of UK law, please notify us by emailing eprints@whiterose.ac.uk including the URL of the record and the reason for the withdrawal request.



eprints@whiterose.ac.uk
<https://eprints.whiterose.ac.uk/>

Orientation of a Diagnostic Ligand Bound to Macroscopically-Aligned Amyloid- β Fibrils Determined by Solid-state NMR

David Townsend, Eleri Hughes, Katie L. Stewart, John M. Griffin, Sheena E. Radford and David A. Middleton*

Dr D. Townsend, Department of Chemistry, Lancaster University, Lancaster LA1 4YB, United Kingdom; d.townsend@lancaster.ac.uk

Dr E. Hughes, Department of Chemistry, Lancaster University, Lancaster LA1 4YB, United Kingdom; elerihughes26@gmail.com

Dr J. Griffin, Materials Science Institute, Lancaster University, Lancaster LA1 4YB, United Kingdom; j.griffin@lancaster.ac.uk

Dr K. Stewart, Department of Physics, Emory University, Atlanta GA 30322; k.l.stewart@emory.edu

Prof. S.E. Radford, Astbury Centre for Structural Molecular Biology, School of Molecular and Cellular Biology, Faculty of Biological Sciences, University of Leeds, Leeds LS2 9JT, United Kingdom; s.e.radford@leeds.ac.uk

*Corresponding author: Prof. D.A. Middleton, Department of Chemistry, Lancaster University, Lancaster, United Kingdom LA1 4YB; d.middleton@lancaster.ac.uk. Telephone: +44 1524 594328

Abstract

With amyloid diseases poised to become a major health burden in countries with ageing populations, diagnostic molecules that aid the detection of amyloid in vitro and in vivo are of considerable clinical value. Understanding how such ligands recognize their amyloid targets would help to design diagnostics that target specific amyloid types associated with a particular disease, but methods to provide comprehensive information are underdeveloped. Here solid-state NMR is used to determine the molecular orientation of the amyloid diagnostic 1-fluoro-2,5-bis[(E)-3-carboxy-4-hydroxystyryl]-benzene (FSB) when bound to fibrils of the Alzheimer's amyloid- β polypeptide aligned on a planar substrate. The ^{19}F NMR spectrum of the aligned complex reveals that FSB is oriented approximately parallel with the fibril long axis and bridges four hydrogen-bonded β -sheets. In addition to providing atomic details to aid the design of amyloid-specific diagnostics, this approach will also illuminate the molecular mechanisms of accessory molecules in amyloid disease.

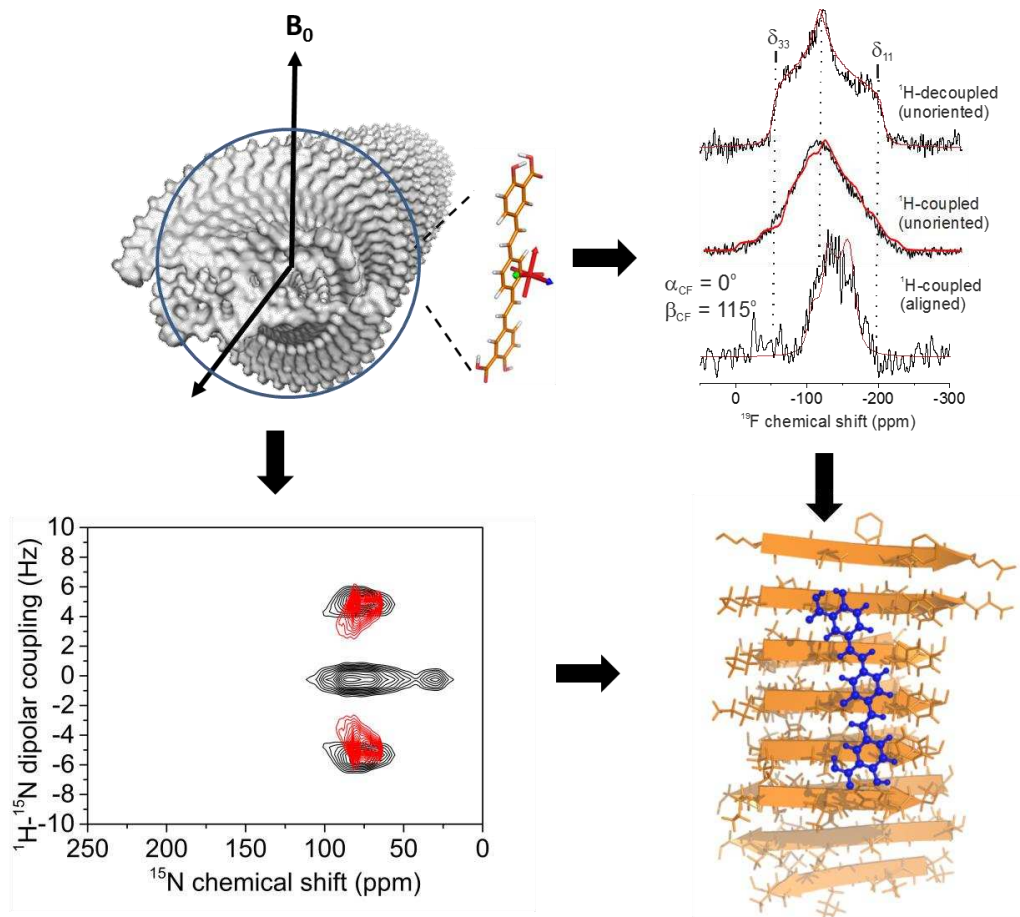


Table of Contents graphic.

The sporadic deposition of insoluble, fibrillar protein-rich deposits within extracellular spaces is associated with several disorders afflicting humans in later life,¹ the archetype being the amyloid- β ($A\beta$) polypeptides associated with Alzheimer's disease.² The atomic details of how proteins self-assemble into amyloid fibrils - central to our mechanistic understanding of amyloid disease - have been revealed by advances in solid-state NMR (SSNMR)³⁻⁸ and cryo-electron microscopy methods⁹ and complete atomic-level models of fibril architectures are now available.^{5, 10-11} To gain a broader understanding of amyloid disorders it is also important to elucidate how biological molecules known to promote fibril formation *in vivo*¹² and diagnostic molecules that detect the formation of amyloid *in vivo* and *in vitro*¹³ recognize and bind to the generic amyloid cross- β motif. Structural insights into ligand binding would cast light on their role in the assembly mechanism and open the door to the tailored design of diagnostics that recognize amyloid from different protein precursors. Atomic details of amyloid-ligand complexes are scant, however, owing to a shortage of high-resolution methods that can determine both the interaction sites and the orientation of ligands within fibrils. Here we demonstrate an approach that exploits SSNMR of macroscopically-aligned fibrils of the 40-amino acid amyloid- β peptide ($A\beta_{40}$) to determine the orientation of a bound diagnostic ligand. When combined with other experimentally-determined restraints, a comprehensive picture of the amyloid-ligand complex is revealed.

Magic-angle spinning (MAS) SSNMR has provided the few available atomic details of amyloid-ligand complexes, such as the binding sites for heparin within $A\beta_{40}$ fibrils¹⁴⁻¹⁵ and the amyloid dye Congo red within the functional prion HET-s(218-289) amyloid.¹⁶ Perturbations of protein chemical shifts or dipolar-driven

polarization transfer between protein and ligand nuclear spins identify the amino acid residues flanking the ligand binding site(s).^{14, 16-17} but do not report on how the ligand aligns on the fibril surface. Ligands may, for example, insert laterally between hydrogen-bonded β -strands, or longitudinally stabilized by side-chain ladders running parallel with the fibril axis (Figure S1, supporting information).

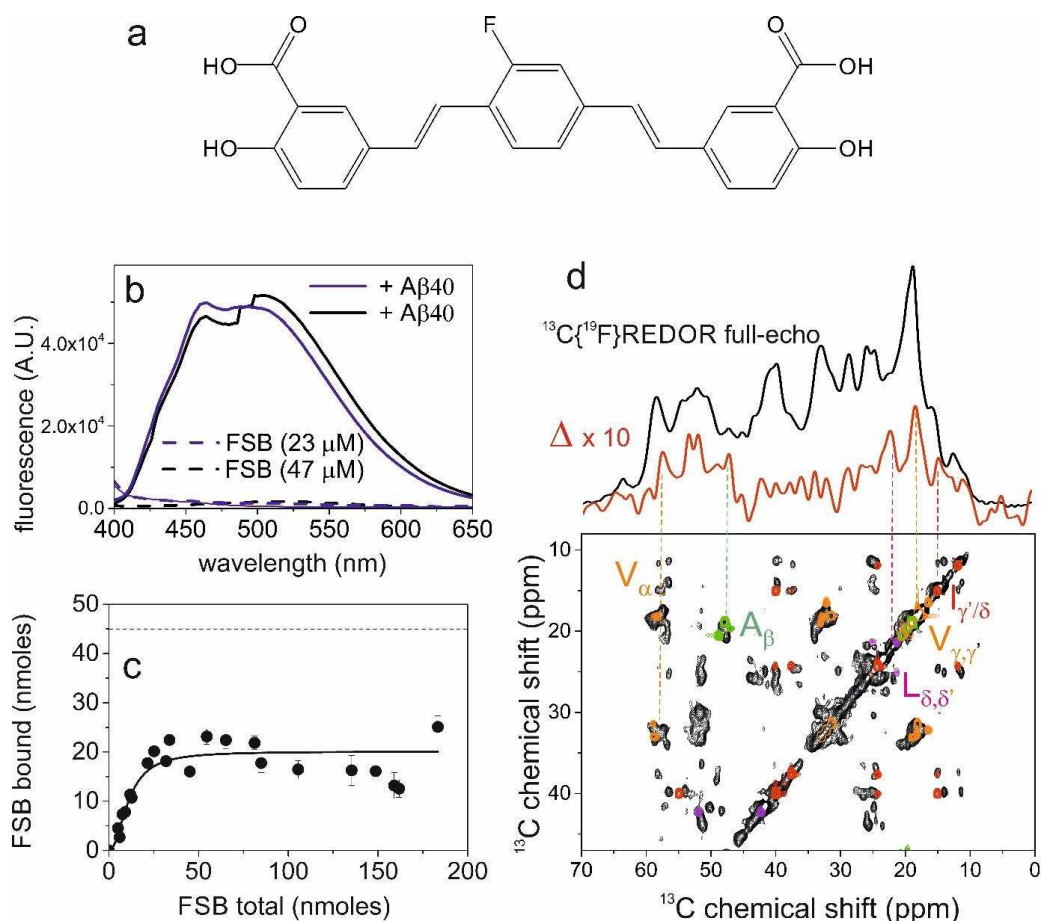


Figure 1. Binding of FSB to [U- ^{15}N , ^{13}C]A β 40 fibrils prepared homogeneously in the 3Q morphology¹⁸⁻¹⁹ (a) Chemical structure of FSB. (b) Fluorescence emission spectrum (with excitation at 360 nm) of FSB in the absence and presence of A β 40 fibrils. (c) Concentration-dependence of FSB binding to fibrils (45 μ M A β 40 monomer equivalent). (d) Detection of close contacts between A β 40 residues in [U- ^{15}N , ^{13}C]A β 40 fibrils and ^{19}F of bound FSB using $^{13}\text{C}\{^{19}\text{F}\}$ REDOR SSNMR. Top: region of a full-echo spectrum (black) obtained without ^{19}F dephasing and a difference spectrum (Δ , with 10-fold vertical expansion) after subtracting a dephased-echo spectrum obtained with a train of 21 π pulses at the ^{19}F frequency. The full REDOR spectra are shown in Figure S3. Bottom: a ^{13}C - ^{13}C spectrum of fibrils (obtained with 20 ms DARR mixing), with labelled peaks assigned as described previously.^{4, 15}

We reasoned that a ligand's binding orientation can be determined by NMR if the insoluble fibrils are aligned in the applied magnetic field. A β 40 fibrils have been partially aligned on planar substrates enabling SSNMR measurements of nuclear spin tensor orientations to refine pre-defined structural models.²⁰ The high length-to-width ratio of amyloid fibrils favors an anisotropic distribution of orientations in which most fibrils lie in the substrate plane.

We tested the theory with the fluorescent amyloid diagnostic ligand 1-fluoro-2,5-bis[(E)-3-carboxy-4-hydroxystyryl]-benzene²¹⁻²² (FSB, Figure 1a), which undergoes a large fluorescence enhancement in the presence of amyloid (Figure 1b). The large chemical shift anisotropy (CSA) of ¹⁹F is a sensitive intrinsic reporter on the molecular orientation of the planar conjugated ring system. Fibrils of uniformly ¹⁵N, ¹³C-labeled A β 40 bound FSB with an association constant K_a of 9.8 μ M and A β 40:FSB stoichiometry of approximately 2:1 at saturation (Figure 1c and Figure S2, a-c). The insoluble fibrils retained strong fluorescence when viewed under a UV lamp (Figure S2d), confirming co-localization of the fibrils and FSB. An intimate contact between FSB and the fibrils was confirmed by a ¹³C-observed {¹⁹F-dephased} rotational-echo double-resonance (REDOR) MAS SSNMR experiment on a 1:2 complex of FSB with [U-¹⁵N,¹³C]A β 40 fibrils (Figure 1d, top). The most prominent peaks in the ¹³C{¹⁹F}REDOR difference spectrum, which correspond to ¹³C sites estimated to be < 6 Å from ¹⁹F of FSB (Figure 1d and Figure S2d), are assigned with reference to a 2D ¹³C-¹³C NMR spectrum (Figure 1d). These sites include Val (C α and C γ/γ'), Ile (C β'/δ), Leu (C δ/δ') and Ala (C α) (Figure 1d, bottom). That selective dephasing is observed in the difference spectrum suggests that FSB occupies specific sites rather than decorating the fibril surface non-specifically.

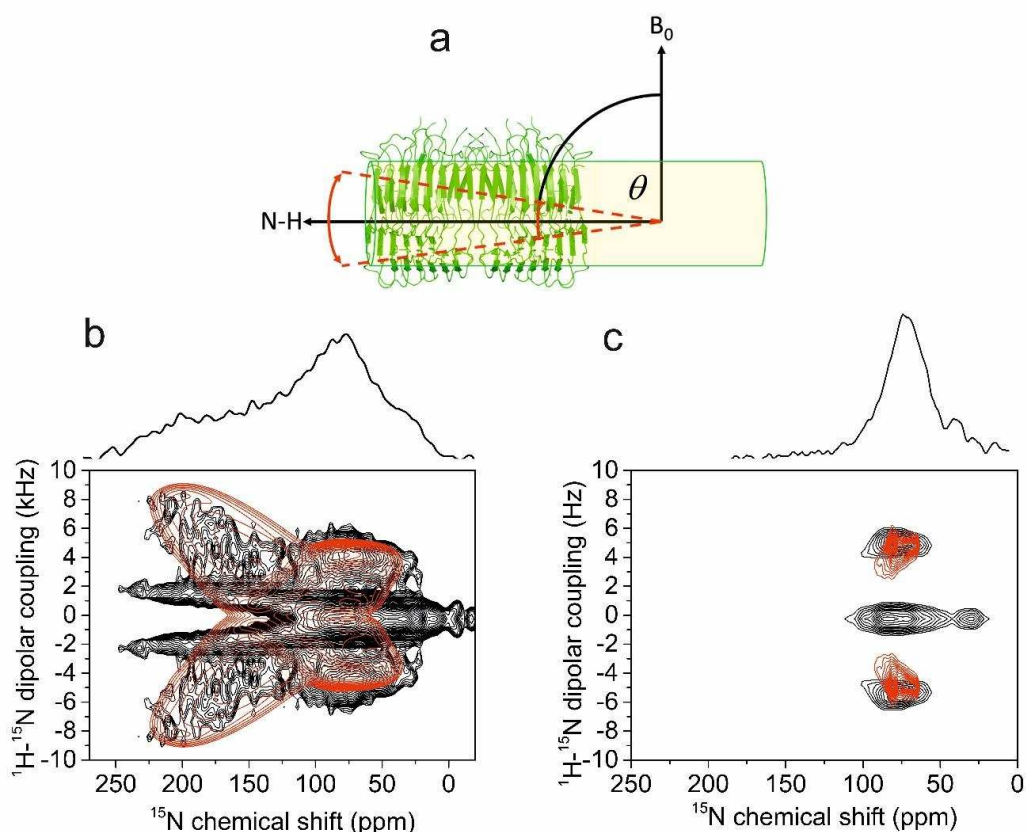


Figure 2. NMR detects the macroscopic alignment of $[\text{U-}^{15}\text{N}, ^{13}\text{C}]\text{A}\beta 40$ fibrils on glass cover slips. B_0 is normal to the plane of the glass surface. (a) When deposited on the planar surface, fibrils (green cartoon) may assume preferred orientations in which the backbone N-H – O=C hydrogen bonds (approximately parallel with the fibril long axis) are oriented at a mean angle θ \pm angle ψ in a Gaussian distribution about the mean. For unoriented fibrils, angle θ takes all values from 0-360°. (b) ^1H - ^{15}N PISEMA spectrum of unoriented hydrated fibrils (black) overlaid with a simulated spectrum (red) for typical backbone ^{15}N chemical shift tensor elements of $\delta_{11} = 223$ ppm, $\delta_{22} = 75$ ppm and $\delta_{33} = 55$ ppm. (c) PISEMA spectrum of fibrils deposited on cover slips overlaid with a simulated spectrum (red) for angles $\theta = 0 \pm 5^\circ$.

The FSB- $[\text{U-}^{15}\text{N}, ^{13}\text{C}]\text{A}\beta 40$ fibril complex was next deposited on a planar substrate of glass cover slips and ^{15}N NMR was used to confirm the fibril alignment. The cover slips were stacked and inserted into an NMR probe-head with a fixed angle, rectangular-wound coil with the applied magnetic field B_0 normal to the plane of the substrate. Randomly-dispersed fibrils were also prepared (in a non-spinning MAS rotor) for comparison. The ^{15}N line shape reflects the degree of fibril alignment, represented by a distribution of fibril orientations on the substrate (or in the MAS rotor) about a mean tilt angle θ relative to B_0 (Figure 2a). The fibrils were visualized

by ^1H - ^{15}N PISEMA NMR, which correlates the anisotropic ^{15}N chemical shift of the peptide backbone amides with the amide N-H dipolar coupling of the same amino acid residue for each molecular orientation. The spectrum of randomly-dispersed fibrils correlates a broad range of chemical shifts and dipolar couplings expected for a powder-like distribution of crystallites (Figure 2b). The spectrum of fibrils on the cover slips is much narrower in both dimensions (Figure 2c) and consistent with a restricted ensemble of fibrils distributed about a tilt angle θ of $85^\circ \pm 5^\circ$ (simulated spectra for fibrils oriented parallel and perpendicular to B_0 are shown in Figure S4).

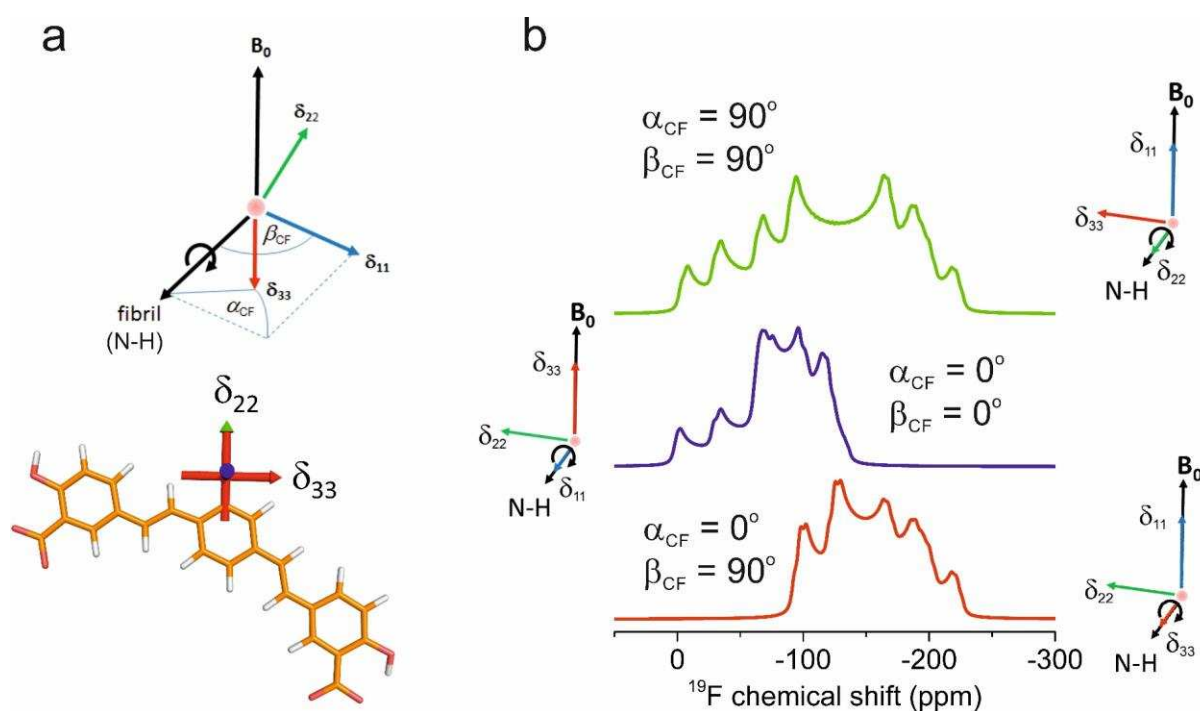


Figure 3. Simulations of ^{19}F NMR spectra of FSB bound to aligned fibrils. (a) The ^{19}F NMR line shape is dependent on the orientations of the principal axes of the ^{19}F chemical shift tensor, $\hat{\delta}_{11}$, $\hat{\delta}_{22}$ and $\hat{\delta}_{33}$, relative to the fibril axis (approximately parallel with the backbone N-H bonds), defined by angles α_{CF} and β_{CF} . The directions of $\hat{\delta}_{11}$, $\hat{\delta}_{22}$ and $\hat{\delta}_{33}$ in the FSB molecular frame (calculated and measured) give the orientation of FSB relative to the fibril axis. (b) Simulated proton-coupled ^{19}F NMR spectra in which each of the principal axes is aligned along the fibril axis.

We developed a theoretical framework to analyse the ^{19}F NMR line shape and determine the orientation of FSB relative to the fibril axis in the aligned FSB-[U- ^{15}N , ^{13}C]A β 40 complex (Figure 3, Supporting Information sections 1.6-1.8 and

Figures S5-S8). ^{19}F NMR spectra were next obtained for the FSB-[U- ^{15}N , ^{13}C]A β 40 complex. Proton-decoupled ^{19}F spectra could be obtained on unoriented fibrils in a non-spinning MAS probe, but for the aligned fibrils ^{19}F -observation with proton-decoupling was not possible using the flat-coil probe. The proton-decoupled spectrum from FSB bound to unoriented fibrils is typical of an axially asymmetric ^{19}F CSA tensor (Figure 3a, top), and the principal values measured by line fitting to the spectrum (Table S1) were used in the subsequent simulations. The proton-coupled spectrum of the same sample was compared with a simulated spectrum based on the measured principal values and the predicted dipolar couplings from the optimised geometry, with no line fitting (Figure 3a, middle). The good agreement between the experimental and simulated line shapes indicates that the predicted couplings and geometry of the dipolar vectors are represented accurately in the calculations. Finally, the proton-coupled ^{19}F NMR spectrum of the oriented FSB-[U- ^{15}N , ^{13}C]A β 40 complex was obtained (Figure 3a, bottom). The spectrum is narrower than that of the unaligned samples and so consistent with restricted orientations of the FSB ligand.

Comparison of the spectrum with simulated spectra for combinations of [α_{CF} , β_{CF}] values from 0 – 180° yielded a two-dimensional array of χ^2 values representing the variance of the experimental and simulated spectra (Figure S8). The closest agreement is found for [$-15^\circ \leq \alpha_{\text{CF}} \leq 30^\circ$] and either [$60^\circ \leq \beta_{\text{CF}} \leq 75^\circ$] or [$115^\circ \leq \beta_{\text{CF}} \leq 130^\circ$]; a representative simulated spectrum (for $\alpha_{\text{CF}} = 0^\circ$, $\beta_{\text{CF}} = 115^\circ$) is overlaid with the experimental spectrum in Figure 4a (bottom; red). This range of angles is consistent with FSB molecules having an approximately longitudinal orientation relative to the fibril axis (Figure S1) and spanning 4 hydrogen

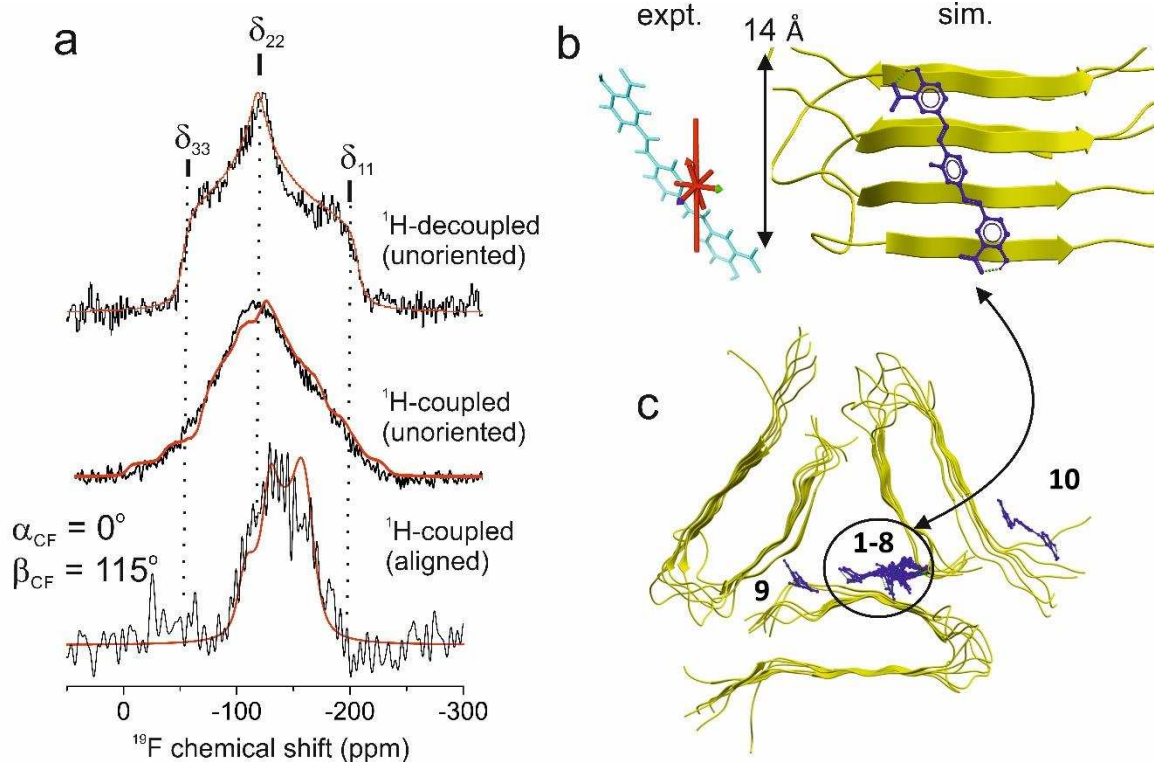


Figure 4. Orientation of FSB when bound to macroscopically aligned $[U-^{15}\text{N}, ^{13}\text{C}]\text{A}\beta 40$ fibrils. (a) Top: proton-decoupled ^{19}F NMR spectrum of FSB bound to unoriented fibrils (in a non-spinning MAS rotor). The best fitting powder line shape obtained by non-linear least squares analysis (red). Middle: Proton-coupled spectrum overlaid with a simulated line shape (red) corresponding to the principal values in Table 1 and the ^1H - ^{19}F coupling constants and geometry for the 4-spin system of FSB. The simulation parameters were not optimised further. Bottom: proton-coupled spectrum of FSB bound to aligned fibrils. The line of best fit corresponds to the angles shown, which define the ^{19}F CSA tensor orientation relative to the vector representing the fibril axis. (b) Orientation of FSB relative to the fibril axis determined experimentally (left) and by docking simulation (representative model). (c) Cross-sectional view of 3Q fibril model (PDB 2LMP) showing FSB (blue) in the 10 lowest energy sites.

bonded β -strands. The lowest-energy docking simulations of FSB with a model of three-fold symmetric $\text{A}\beta 40$ fibrils (PDB 2LMP) concur with this orientation (Figure 4b). A similar orientation has been proposed for thioflavin T, with the ligand binding along surface side-chain grooves running parallel to the fibril axis.¹³ FSB must occupy two longitudinal sites in order to account for the measured $\text{A}\beta 40$:FSB stoichiometry of 2:1. The 8 lowest-energy docking models suggest a primary binding site at the innermost face of the C-terminal β -sheet, close to Ile, Val and Leu residues identified by REDOR NMR (Figures 4c and S9) and which form a

hydrophobic ladder to stabilise the ligand. Several lower-energy models (e.g. 9 and 10 in Figure 3c) may represent the secondary site.

In summary, we demonstrate a direct NMR method for detecting the orientation of ligand molecules when bound to the surface of amyloid fibrils. Transferred Overhauser enhancements and residual dipolar couplings in solution have also been applied in this context,²³⁻²⁴ but these are less suitable when ligands are bound tightly to insoluble fibrils. Our approach is applicable to other diagnostic amyloid-binding molecules such as PET ligands²⁵ and can provide new insights into the binding properties of physiological ligands such as glycosaminoglycans, which bind tightly to amyloid. With appropriate isotope labelling of molecules with no intrinsic reporter nucleus, this method combined with other MAS SSNMR measurements,¹⁷ can provide much more detailed atomic models with which to guide the design of molecules targeting specific amyloid types.

Acknowledgements: We thank S. Linse and D. Walsh for the gift of the A β 40 expression clone. Funding was provided by BBSRC (UK) Grants BB/K01451X/1 and BB/K015958/1. Additional funding was provided by British Heart Foundation Project Grant PG/16/18/32070. We acknowledge support from CCP-NC, funded by EPSRC (EP/M022501/1), and the UKCP consortium, funded by EPSRC (EP/P022561/1). We are grateful to the UK Materials and Molecular Modelling Hub for computational resources, which is partially funded by EPSRC (EP/P020194).

Supporting Information

All experimental methods, tables of data, supplementary figures and additional references.

References

1. Knowles, T. P. J.; Vendruscolo, M.; Dobson, C. M., The amyloid state and its association with protein misfolding diseases. *Nature Reviews Molecular Cell Biology* **2014**, 15 (6), 384-396.
2. Selkoe, D. J.; Hardy, J., The amyloid hypothesis of Alzheimer's disease at 25years. *EMBO Mol. Med.* **2016**, 8 (6), 595-608.
3. Meier, B. H.; Riek, R.; Bockmann, A., Emerging Structural Understanding of Amyloid Fibrils by Solid-State NMR. *Trends Biochem. Sci.* **2017**, 42 (10), 777-787.
4. Petkova, A. T.; Ishii, Y.; Balbach, J. J.; Antzutkin, O. N.; Leapman, R. D.; Delaglio, F.; Tycko, R., A structural model for Alzheimer's beta-amyloid fibrils based on experimental constraints from solid state NMR. *Proc. Natl. Acad. Sci. U. S. A.* **2002**, 99 (26), 16742-16747.
5. Walti, M. A.; Ravotti, F.; Arai, H.; Glabe, C. G.; Wall, J. S.; Bockmann, A.; Guntert, P.; Meier, B. H.; Riek, R., Atomic-resolution structure of a disease-relevant A beta(1-42) amyloid fibril. *Proc. Natl. Acad. Sci. U. S. A.* **2016**, 113 (34), E4976-E4984.
6. Schutz, A. K.; Vagt, T.; Huber, M.; Ovchinnikova, O. Y.; Cadalbert, R.; Wall, J.; Guntert, P.; Bockmann, A.; Glockshuber, R.; Meier, B. H., Atomic-Resolution Three-Dimensional Structure of Amyloid beta Fibrils Bearing the Osaka Mutation. *Angewandte Chemie-International Edition* **2015**, 54 (1), 331-335.
7. Colvin, M. T.; Silvers, R.; Frohm, B.; Su, Y. C.; Linse, S.; Griffin, R. G., High Resolution Structural Characterization of A beta(42) Amyloid Fibrils by Magic Angle Spinning NMR. *J. Am. Chem. Soc.* **2015**, 137 (23), 7509-7518.
8. Colvin, M. T.; Silvers, R.; Ni, Q. Z.; Can, T. V.; Sergeev, I.; Rosay, M.; Donovan, K. J.; Michael, B.; Wall, J.; Linse, S.; Griffin, R. G., Atomic Resolution Structure of Monomorphic A beta(42) Amyloid Fibrils. *J. Am. Chem. Soc.* **2016**, 138 (30), 9663-9674.
9. Gremer, L.; Scholzel, D.; Schenk, C.; Reinartz, E.; Labahn, J.; Ravelli, R. B. G.; Tusche, M.; Lopez-Iglesias, C.; Hoyer, W.; Heise, H.; Willbold, D.; Schroder, G. F., Fibril structure of amyloid-beta(1-42) by cryo-electron microscopy. *Science* **2017**, 358 (6359), 116-+.
10. Fitzpatrick, A. W. P.; Debelouchina, G. T.; Bayro, M. J.; Clare, D. K.; Caporini, M. A.; Bajaj, V. S.; Jaroniec, C. P.; Wang, L. C.; Ladizhansky, V.; Muller, S. A.; MacPhee, C. E.; Waudby, C. A.; Mott, H. R.; De Simone, A.; Knowles, T. P. J.; Saibil, H. R.; Vendruscolo, M.; Orlova, E. V.; Griffin, R. G.; Dobson, C. M., Atomic structure and hierarchical assembly of a cross-beta amyloid fibril. *Proc. Natl. Acad. Sci. U. S. A.* **2013**, 110 (14), 5468-5473.
11. Nelson, R.; Sawaya, M. R.; Balbirnie, M.; Madsen, A. O.; Riek, C.; Grothe, R.; Eisenberg, D., Structure of the cross-beta spine of amyloid-like fibrils. *Nature* **2005**, 435 (7043), 773-778.
12. Quittot, N.; Sebastiao, M.; Bourgault, S., Modulation of amyloid assembly by glycosaminoglycans: from mechanism to biological significance. *Biochem. Cell Biol.* **2017**, 95 (3), 329-337.
13. Biancalana, M.; Koide, S., Molecular mechanism of Thioflavin-T binding to amyloid fibrils. *Biochimica Et Biophysica Acta-Proteins and Proteomics* **2010**, 1804 (7), 1405-1412.
14. Stewart, K. L.; Hughes, E.; Yates, E. A.; Akiyama, G. R.; Huang, T. Y.; Lima, M. A.; Rudd, T. R.; Guerrini, M.; Hung, S. C.; Radford, S. E.; Middleton, D. A., Atomic Details of the Interactions of Glycosaminoglycans with Amyloid-beta Fibrils. *J. Am. Chem. Soc.* **2016**, 138 (27), 8328-8331.

15. Madine, J.; Pandya, M. J.; Hicks, M. R.; Rodger, A.; Yates, E. A.; Radford, S. E.; Middleton, D. A., Site-specific identification of an A-beta fibril-heparin interaction site by using solid-state NMR spectroscopy. *Angew. Chemie. Int. Ed.* **2012**, 51 (52), 13140-13143.
16. Schutz, A. K.; Soragni, A.; Hornemann, S.; Aguzzi, A.; Ernst, M.; Bockmann, A.; Meier, B. H., The Amyloid-Congo Red Interface at Atomic Resolution. *Angewandte Chemie-International Edition* **2011**, 50 (26), 5956-5960.
17. Herrmann, U. S.; Schutz, A. K.; Shirani, H.; Huang, D. Z.; Saban, D.; Nuvolone, M.; Li, B.; Ballmer, B.; Aslund, A. K. O.; Mason, J. J.; Rushing, E.; Budka, H.; Nystrom, S.; Hammarstrom, P.; Bockmann, A.; Cafilisch, A.; Meier, B. H.; Nilsson, K. P. R.; Hornemann, S.; Aguzzi, A., Structure-based drug design identifies polythiophenes as antiprion compounds. *Sci. Transl. Med.* **2015**, 7 (299), 17.
18. Petkova, A. T.; Leapman, R. D.; Guo, Z. H.; Yau, W. M.; Mattson, M. P.; Tycko, R., Self-propagating, molecular-level polymorphism in Alzheimer's beta-amyloid fibrils. *Science* **2005**, 307 (5707), 262-265.
19. Stewart, K. L.; Hughes, E.; Yates, E. A.; Middleton, D. A.; Radford, S. E., Molecular Origins of the Compatibility between Glycosaminoglycans and A beta 40 Amyloid Fibrils. *J. Mol. Biol.* **2017**, 429 (16), 2449-2462.
20. Oyler, N. A.; Tycko, R., Absolute structural constraints on amyloid fibrils from solid-state NMR spectroscopy of partially oriented samples. *J. Am. Chem. Soc.* **2004**, 126 (14), 4478-4479.
21. Sato, K.; Higuchi, M.; Iwata, N.; Saido, T. C.; Sasamoto, K., Fluoro-substituted and C-13-labeled styrylbenzene derivatives for detecting brain amyloid plaques. *Eur. J. Med. Chem.* **2004**, 39 (7), 573-578.
22. Velasco, A.; Fraser, G.; Delobel, P.; Ghetti, B.; Lavenir, I.; Goedert, M., Detection of filamentous tau inclusions by the fluorescent Congo red derivative FSB (trans,trans)-1-fluoro-2,5-bis(3-hydroxycarbonyl-4-hydroxy)styrylbenzene. *FEBS Lett.* **2008**, 582 (6), 901-906.
23. Chen, Z. J.; Krause, G.; Reif, B., Structure and orientation of peptide inhibitors bound to beta-amyloid fibrils. *J. Mol. Biol.* **2005**, 354 (4), 760-776.
24. Ivancic, V. A.; Ekanayake, O.; Lazo, N. D., Binding Modes of ThioflavinT on the Surface of Amyloid Fibrils Studied by NMR. *Chemphyschem* **2016**, 17 (16), 2461-2464.
25. Sabri, O.; Sabbagh, M. N.; Seibyl, J.; Barthel, H.; Akatsu, H.; Ouchi, Y.; Senda, K.; Murayama, S.; Ishii, K.; Takao, M.; Beach, T. G.; Rowe, C. C.; Leverenz, J. B.; Ghetti, B.; Ironside, J. W.; Catafau, A. M.; Stephens, A. W.; Mueller, A.; Koglin, N.; Hoffmann, A.; Roth, K.; Reiningger, C.; Schulz-Schaeffer, W. J.; Florbetaben Phase 3 Study, G., Florbetaben PET imaging to detect amyloid beta plaques in Alzheimer's disease: Phase 3 study. *Alzheimers & Dementia* **2015**, 11 (8), 964-974.